

Comparison of Seismic Performance Improvement Techniques of End Plate Connections through Intentionally Weakening of Beam

Vahid Bahaari Zargar¹, Mohsen Gerami^{2*}, and Mohammad Bahirai³

1. M.Sc. Graduate, Earthquake Department, Faculty of Civil Engineering, Semnan University, Semnan, Iran

2. Professor, Earthquake Department, Faculty of Civil Engineering, Semnan University, Semnan, Iran, *Corresponding Author; email: mgerami@semnan.ac.ir

3. Ph.D. Graduate, Earthquake Department, Faculty of Civil Engineering, Semnan University, Semnan, Iran

Received: 30/09/2019

Accepted: 29/05/2021

ABSTRACT

In some cases, such as provisions changes in new code or even changes in the structure performance of the building, it may be probable that the component thickness of end plate steel frame connections does not qualify related regulations. In these conditions, there is a need to improve the performance of the connection for preventing the plastic hinge from occurring at the steel column face. For this purpose, two general techniques are accessible that include intentionally weakening the beam through “reduction” and “annealing”. The latter process is a heat induction technique meant to reduce the yield and tensile strength of steel. The current research is about to compare these two techniques and address the parameters influencing the performance of “the enhanced connection”. For each technique, four specimens having end plates with different thicknesses are considered. It is concluded that the heat induction technique was preferable in terms of energy dissipation, moment capacity, local buckling of beam and torsional stability. It should be noted that both techniques were successful in shifting the plastic hinge action away from the column face for the endplate connections with a maximum decrease of 15 mm in the endplate thickness. Moreover, eight numerical models were investigated to compare the “heat induction” and the “reduction” techniques sensitivity to temperature of the weakened and width of the trimmed region respectively.

Keywords:

Seismic performance enhancement;
Extended endplate connections;
Heat-treatment method

Highlights

- “Annealing” and “reduction” methods are compared as two improvement techniques for end plate connection with an imperfection in end plate thickness.
- The heat induction technique was preferable in terms of energy dissipation, moment capacity, local buckling of beam and torsional stability
- Both techniques were successful in shifting the plastic hinge action away from the column face for the endplate connections with a maximum decrease of 15 mm in the endplate thickness.
- “Reduction” technique sensitivity to the width of the trimmed area was more than “annealing” technique sensitivity to temperature of weakened area

1. Introduction

After the 1994 Northridge earthquake, researches

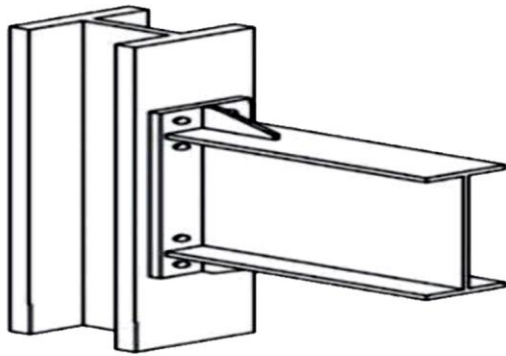
showed that most of the damages in the area of connection are due to a brittle welding fracture and a lack of connection ductility. Two ideas were proposed by Engelhardt and Sabol [1] and other researchers to solve this problem and improve the seismic performance of the connections. The first idea is to strengthening the connection, in which plastic hinge promotes far from the connection. One of the strengthening strategies is the use of stiffeners, side plates, and haunches. The second idea is the intentional weakening of the beam at a distance of the column face. This technique promotes development of the beam plastic hinge away from the welded joint. The most common weakening method of the beam is RBS (Reduced Beam Section). Sophianopoulos and Deri [2] presented an optimization procedure using standard procedures of Mechanics, advance regression analyses and numerical procedure for achieving best beam-to-column reduced beam section connections in steel moment frames under static loading. An idea was recently proposed for promoting the plastic hinge far from the connections by Morrison et al. [3]. The method involves reducing the strength of specified regions of the beam flanges by exposing them to 1050°C with the rate of 7.2°C/min, holding this temperature for 15 minutes, and followed by slow cooling with the rate of 0.33°C/min. This special process of heating is called annealing. This process has been designed to reduce the yield and tensile strength of A992 steel by approximately 35% and 25%, respectively.

Further studies conducted to improve the seismic performance of the end plate connections by researchers. Uang et al. [4] demonstrated by studying RBS methods for rehabilitate steel moment connection, RBS to the beam bottom flange, which was accompanied by removing steel backing and weld tabs, could not prevent brittle fracture of the low-toughness groove welded joint in the top flange. Judd et al. [5] studied a new technique for seismic rehabilitation of Pre-Northridge connections based on T-stub connectors. The result showed that the gravity frame retrofitted through such technique can be used in seismic prone regions. Morkhade et al. [6]

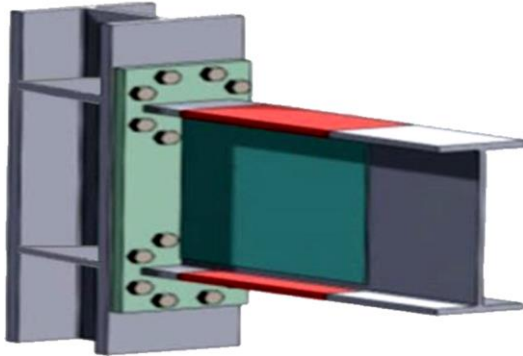
investigated the effect of web opening on flexural behavior of hybrid beam. The results of investigations revealed that using the web opening has increased the strength of hybrid beam by more than 40%. Kim and Lee [7] conducted an experimental study on improved Pre-Northridge connection by haunches on beam bottom flange. In this study, haunches caused the plastic hinge promoted far from the strengthened area and plastic rotation capacity exceeded 4% rad. T-stub connection under out-of-plane bending was investigated by Gil and Goñi [8]. It was concluded from this study, bending capacity and initial rotational stiffness of the connection satisfied the Eurocode 3 limits. Han et al. [9] demonstrated the available rotation capacity decreases with the end plate thickness. Thus, the bolts, are likely to fail before the end-plate, which behaves in a ductile manner. Gerami et al. [10] noticed an increased participation in the connection components when the pitch distance was increased between the bolt and the beam flange. They also observed change in the failure mode based on the arrangement of the bolts for T-stub connection. Abidelah et al. [11] with studying the behavior of eight bolted connections with and without stiffener showed, the stiffening of the end-plate gives a significant increase in the moment resisting capacity and the initial stiffness but lead to a reduction of the connection ductility.

2. Improved Extended End Plate Connection (BEEP) through Annealing

According to studies conducted after the 1994 Northridge earthquake, five connections were prequalified by AISC 358 [12] to improve the seismic performance of the connections. One out of these five prequalified connections is a bolted extended end plate moment connection (BEEP). According to Figure (1), this connection with three changes has been investigated experimentally to improve its seismic performance by Quayyum [13]. The first of the three performance enhancing modifications was the removal of the end plate stiffener to avoid a high stress concentration between stiffener and end plate and rearrangement of the bolts in a hexagonal pattern.



(a) Bolted Extended end Plate Moment Connection [11]



(b) Proposed Connection by Quayyum et al [12]

Figure 1. Three changes applied to BEEP connection by Quayyum [13].

The second modification was welding a steel plate to the beam web and end plate in the expected plastic hinge region which stiffens the beam web and delays the onset of web local buckling. The third modification was involved intentionally weakening the beam flanges through “annealing” technique to promote plastic hinge to predefined area in the beam. In “heat induction” technique through annealing the beam flanges at the certain distance from the column, low stress demands in near weld region was experienced. Moreover, from comparison of both post-test simulations (with and without the web stiffener) it was observed that, web stiffener increases the moment capacity and slows the initial rate of strength degradation between 3% and 4% interstory drift and heat induction did not have significant effect

on the welding of the web stiffener [13].

The main purpose of this study is to compare the “annealing” and “reduction” techniques to improve end plate connection performance with an imperfection in the end plate thickness. The proposed connection by Quayyum [13] was selected for the current study due to the experimental results obtained to improve the seismic performance of the extended end plate connection (Figure 1b).

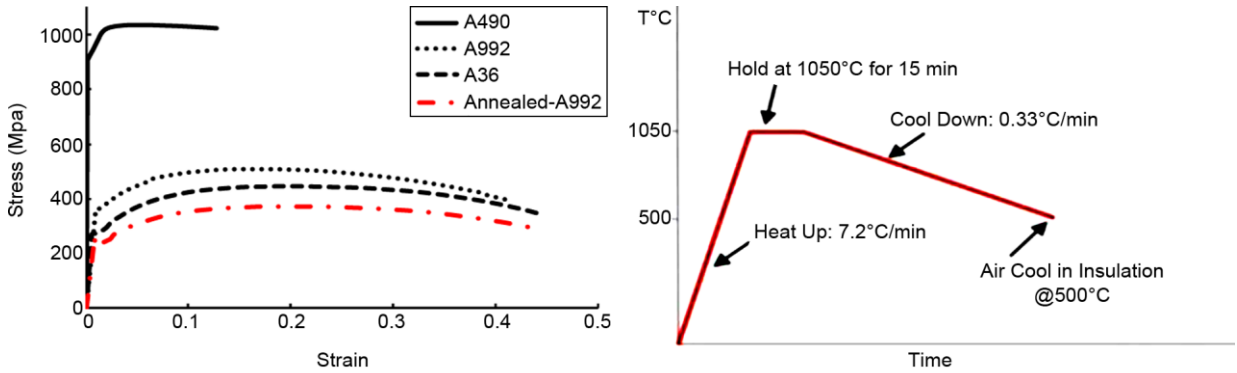
3. Verification of finite element models

In this study, the numerical results of the proposed connection by Quayyum [13] are compared with the experimental results to verify the accuracy of the FE models. Considering the reference connection of both the “annealing” and “reduction” techniques is considered identical, only the verification of the “heat induction” model is presented. A brief description of the finite element modeling details is presented next.

1. FE Software ABAQUS [14] is used to model this connection. The mechanical properties of all component materials are taken from the experimental specimens mentioned in Table (1). The stress-strain response of the materials in plastic area and temperature history of Annealed-A992 is presented in Figure (2).
2. As shown in Figure (3), the dimensions and geometry of the beam, column and connection components are exactly modeled in accordance with the experimental specimens.
3. Contact between the end plate and column, bolts and end plate, bolts and column are defined from two components, perpendicular-to-surface and tangent-to-surface, while only tangent-to-surface is used to contact between the bolts and holes. To consider the frictional forces, Coulomb's coefficient is assumed to be 0.3 that is the middle of the range 0.15 to 0.6,

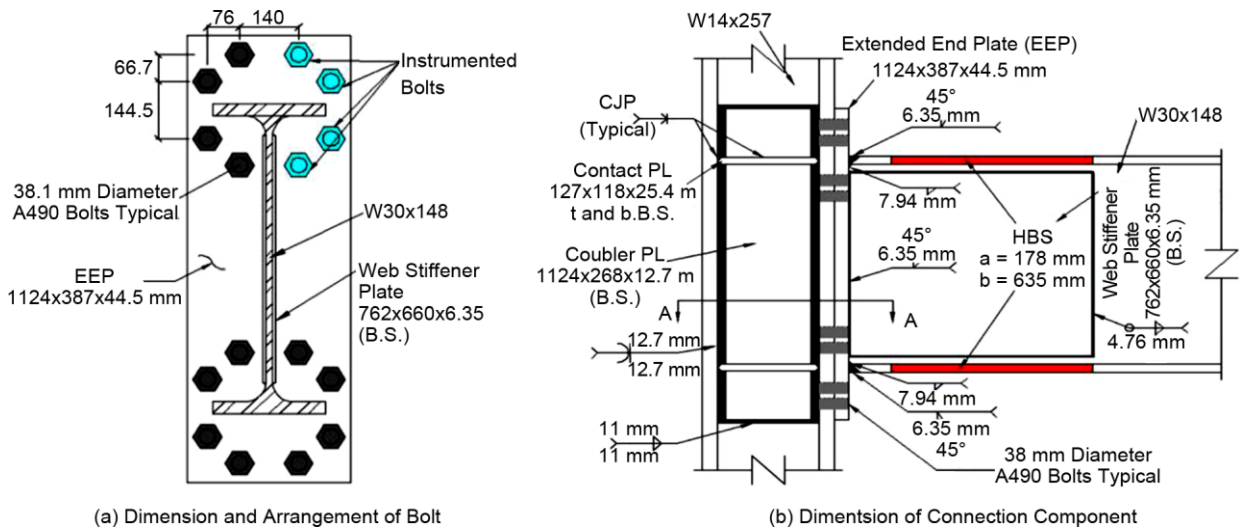
Table 1. Material properties used in specimens to validate numerical and experimental results [12].

Components	Material	Young's Modulus (Mpa)	Yielding Strength (Mpa)	Ultimate Strength (Mpa)	Ultimate Strain	Poisson's Ratio
Column and Beam	A992	200000	360	508	0.42	0.3
End Plate	A36	187000	270	450	0.4	0.26
Bolt	A490	210000	850	995	0.14	0.3
Heated Part	Anealed-A992	200000	234	330	0.45	0.3



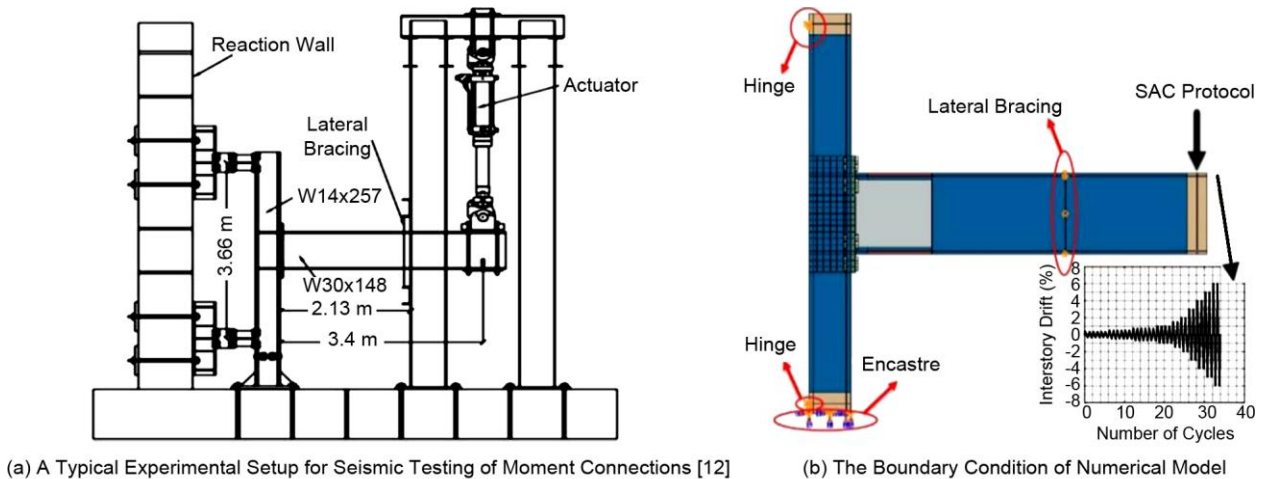
(a) Stress-Strain Response of the Materials in Plastic Area (b) Temperature History of Annealed-A992

Figure 2. Material properties used in specimens [2].



(a) Dimension and Arrangement of Bolt (b) Dimension of Connection Component

Figure 3. The dimensions and geometry of the beam, column and connection components [12].



(a) A Typical Experimental Setup for Seismic Testing of Moment Connections [12] (b) The Boundary Condition of Numerical Model

Figure 4. Loads and boundary conditions.

which is defined for steel surfaces. The end plate and beam are connected by a complete joint penetration (CJP) groove and a fillet welds, these two parts are considered to be continuous in the FE model.

4. As shown in Figure (4), the load is applied in two steps. First, bolt pre-tension is applied in accordance with AISC LRFD specification [15]. Then, main loads were applied at the beam tip in accordance with SAC/BD-97/02 [16] and

consisted of quasi-static increasing displacement cycles. The prescribed displacements included six cycles of 0.375, 0.5 and 0.75% interstory drift, followed by four cycles of 1% interstory drift and two cycles each of 1.5, 2, 3, 4, 5, 6% and so forth interstory drift. Moreover, the boundary conditions were applied such that it mimics the boundary conditions applied in the experimental setup for conventional seismic testing of moment connections.

- Based on the mesh sensitivity analysis performed on the FE model, mesh size varied from 8 to 25 cm in the components. A finer mesh was considered along the beam and column length in the vicinity of the beam-to-column connection, and also in the column panel zone where the majority of the inelastic action occurs (Figure 5). The bolts and end plate was also discretized with finer mesh for accurate prediction of the connection behavior. The other regions of the connection will remain elastic, and hence, coarser mesh was used in those places to reduce the computational time and cost. For this connection, the shape of the element is hexahedral and also structured mesh

is selected for them.

Moment–rotation hysteretic curves of the connection for both experimental and simulation specimens are shown in Figure (6). The FEA prediction is in a good overall agreement with the experiment response both in terms of peak strength prediction and the rate of strength degradation. The predicted deflected shape is compared with a photograph of the test specimen at the end of loading in Figure (7). These comparisons show that local deformations including buckling modes are reasonably predicted by the FEA model.

Figure (8) illustrates the progression of inelastic action along the beam flange via bar graphs in which the distribution of longitudinal tensile strains (normalized by the yield strain) along the center-line of the beam flange at various stages of the loading history are plotted. These plots illustrate the influence of the HBS in promoting majority of the inelastic action away from the beam flange to end plate connection. The red and blue bars indicate the longitudinal strain at a distance from the end of weakened region to the column face for the experimental and FEM specimens respectively.

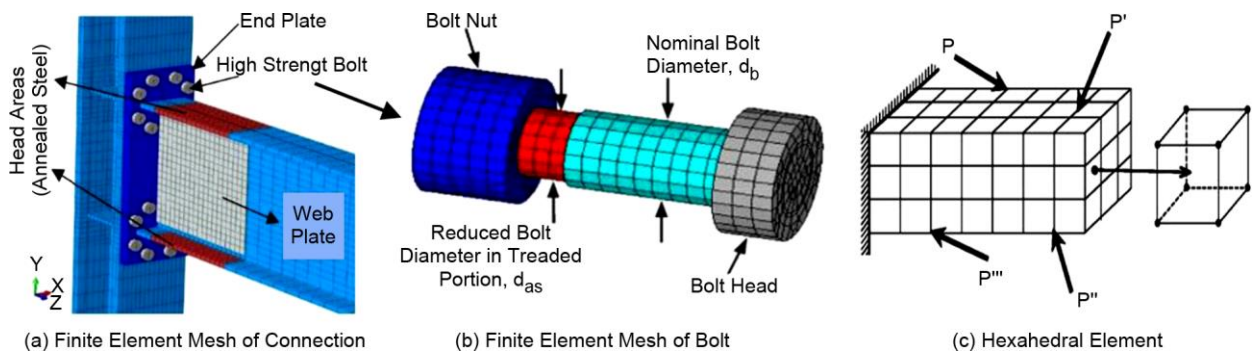


Figure 5. Finite element mesh of connection component.

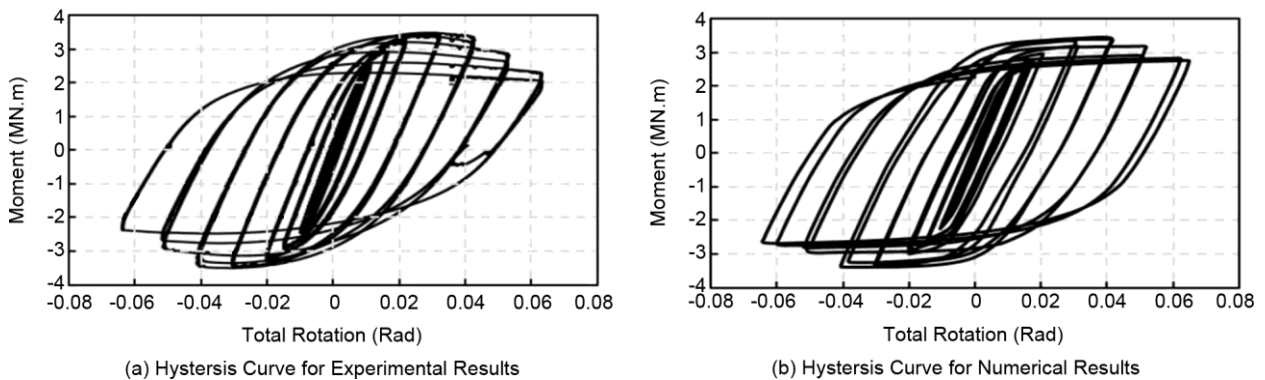


Figure 6. Hysteresis curves of numerical models and experimental specimens.

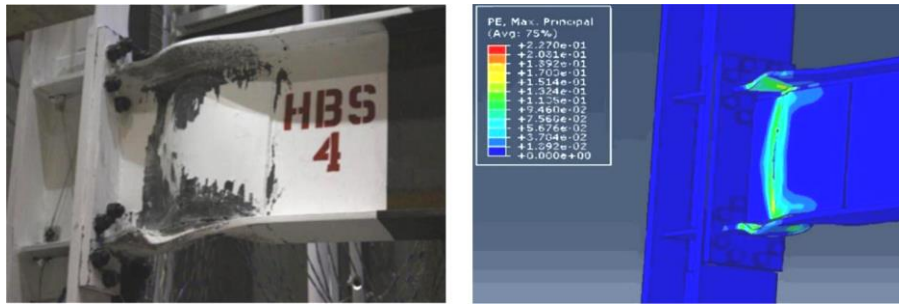


Figure 7. View of experimental and numerical specimens [12].

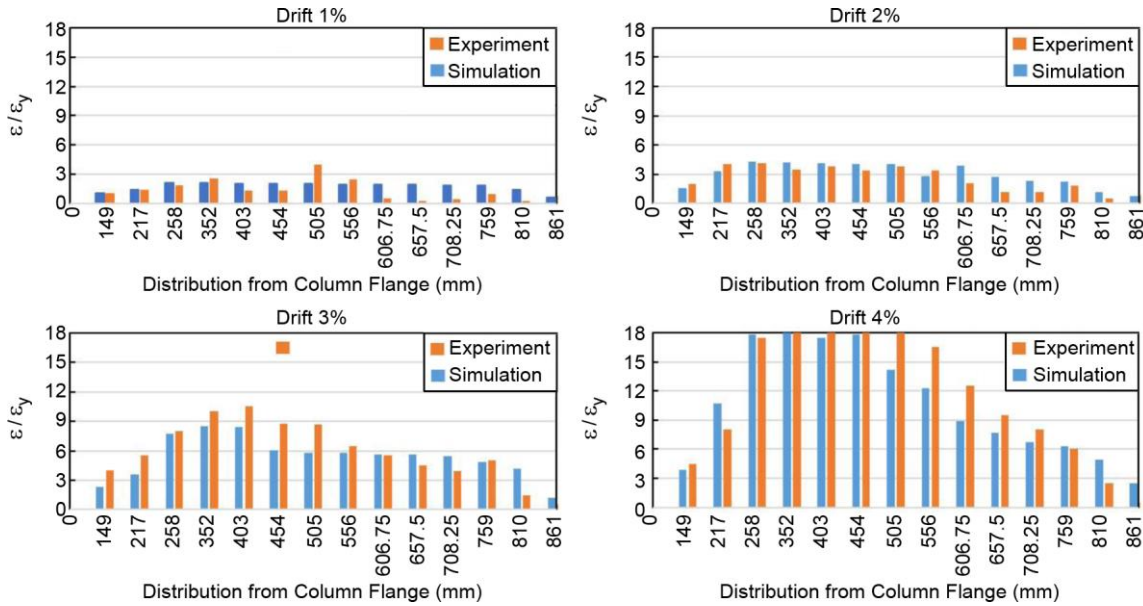


Figure 8. The comparison between FEM and experimental results of longitudinal strain along the center of top flange of the beam from proposed connection.

As loading is continued, the longitudinal strain increased more in the heat treated areas than unheated regions adjacent to the beam flange to end plate welds. This demonstrates that the large displacements imposed at the beam tip are mostly accommodated by flexural deformation in the HBS region. It is important to note that the beam length of 3.4 m (134 in) used in this study corresponds to a moment frame with a clear span of 6.8 m (22 feet). This relatively short span results in a large moment gradient, which is reflected in the strain profiles.

4. Improve the Performance of Endplate Connection with an Imperfection through “Annealing” and “Reduction” Techniques

Seismic performance improvement of existing steel structures is an inevitable work in the cases of the provisions changes in new code or even

changes in the structure performance of the building. The unforeseen changes can increase the applied load, and consequently the probability of damages in building. In some cases, the thickness of endplate would be less than the required value. In this paper, “annealing” and “reduction” techniques are compared as two improvement methods for the endplate connections with imperfection in end plate thickness. For this purpose, one reference specimens and three other specimens of proposed end plate connections with the same properties of connections components and different thickness of end plate for each technique are modeled (see Table 2). As shown in Table (2), the improved specimens with “annealing” and “reduction” techniques were named HBS (Heat-treated beam section) and RBS (Reduced Beam Section) respectively. The radius-cut is used in beam flange for “reduction”

technique. The end plate thickness of three specimens is considered 25, 30 and 35 mm for “annealing” and “reduction” specimens. The results obtained by the numerical analyses are presented in three parts. Each part is discussed in more detail later and a brief review of them is tabulated in Table (3).

4.1. Global Response of HBS and RBS Specimens

Figure (9) shows moment-rotation numerical results of HBS and RBS specimens. These global responses of specimens show that the HBS specimens with wide hysteresis loop indicating better energy dissipation compared with RBS specimens. However, the moment-rotation results for both HBS and RBS specimens with the end plate thickness of 25 mm are nearly equal (see

Figure 9g and 9h). Moreover, the pinching of all moment-rotation curves is increased with decreasing the endplate thickness. This relates to the increase in plasticity and permanent deformation in specimens. Also it can be seen that a 20 mm reduction in the endplate thickness in specimen EP-HBS-Th25 and EP-RBS-Th25 relative to the reference specimens resulted in a 12% and 4% reduction in moment capacity of the connection, respectively. This is probably due to the occurrence of a stress concentration and subsequently premature failure in the endplate region. Moreover, the connection elastic stiffness of all specimens is decreased with a 20 mm reduction in the endplate thickness, while beam weakening technique increased plastic stiffness of the specimens as shown in Table (3).

Table 2. Summary of the numerical model details.

Group	Specimens	a (cm)	b (cm)	c (mm)	T _{HBS} (°C)	t _{pl} (cm)
Reference Connection	EP-HBS-Ref	17.8	63.5	-	1000	45
HBS Specimens with Imperfection	EP-HBS-Th35	17.8	63.5	-	1000	35
	EP-HBS-Th30	17.8	63.5	-	1000	30
	EP-HBS-Th25	17.8	63.5	-	1000	25
Reference Connection	EP-RBS-Ref	17.8	63.5	50	-	45
RBS Specimens with Imperfection	EP-RBS-Th35	17.8	63.5	50	-	35
	EP-RBS-Th30	17.8	63.5	50	-	30
	EP-RBS-Th25	17.8	63.5	50	-	25

a: Weakened area distance from column

b: Weakened area length

c: Reduced area diameter for RBS connection

T_{pl}: End plate thickness

T_{HBS}: Maximum temperature of weakened area for HBS connection

Table 3. Finite element results: moment resistance capacity, initial rotational stiffness, end plate deformation and failure mode.

Specimens	M _{max} (KN.m)	$\frac{M_{max}}{M_{max}(EP-HBS-Ref/EP-RBS-Ref)}$	M _y (KN.m)	θ _y (rad×10 ⁻⁴)	R _{in} =M _y /θ _y (MN.m/rad)	D _x (mm)	D _y (mm)	F ^N
EP-HBS-Ref	3420	1	2235	76	294	4.7	0.29	a
EP-HBS-35	3200	0.93	2038	72	283	7.4	0.73	a
EP-HBS-30	3250	0.95	2083	71	293	13.5	3.2	a
EP-HBS-25	3050	0.89	1906	68	280	17	3.8	b
EP-RBS-Ref	2860	1	1833	83	220	2.3	0.32	a
EP-RBS-35	3190	1.1	2084	79	264	7.2	1.4	a
EP-RBS-30	3140	1.09	2107	77	274	13.4	3.1	a
EP-RBS-25	3050	1.07	1990	74	269	16.6	3.8	b

a: Plastic hinge in the beam

b: Plastic hinge in the end plate

^N: Failure mode

D_x: Maximum horizontal deformation of the end plate along its height

D_y: Maximum vertical deformation of the end plate along its width

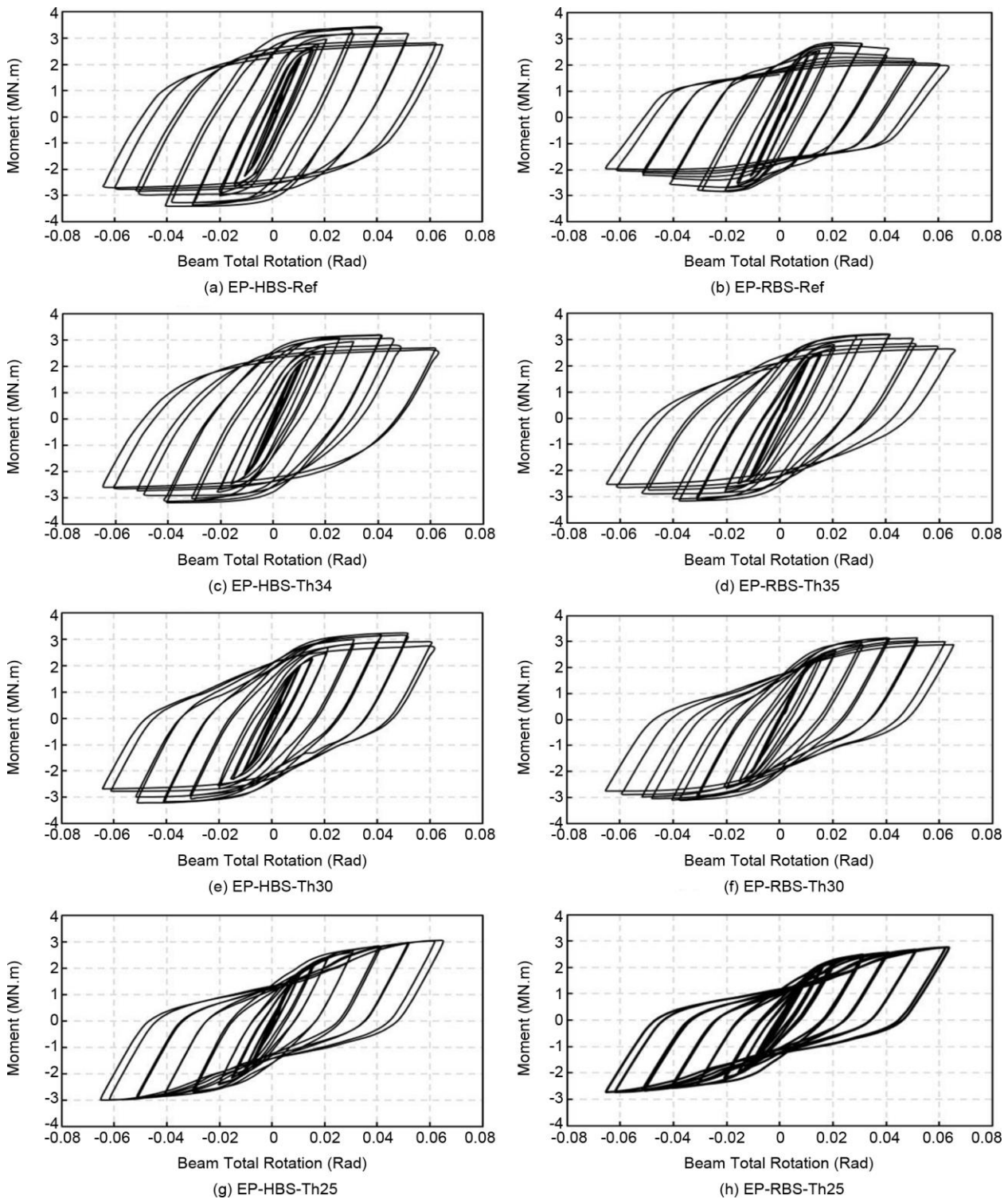


Figure 9. Hysteresis curves of HBS and RBS specimens.

4.2. Plastic Hinge Formation in HBS and RBS Specimens

Figure (10) illustrates longitudinal tensile strains (normalized by the yield strain) at a distance of 861 mm from the column and along the center of the beam flange at the end of loading. The reason for selecting this distance was to find

the impact of the intentional weakening of the beam in the behavior of connection. The bars highlighted in red, blue and black represent the strains in heat-treated regions in HBS specimens, reduced section of RBS specimens and non-weakened region respectively. It can be seen that, by reducing the thickness of endplate for both

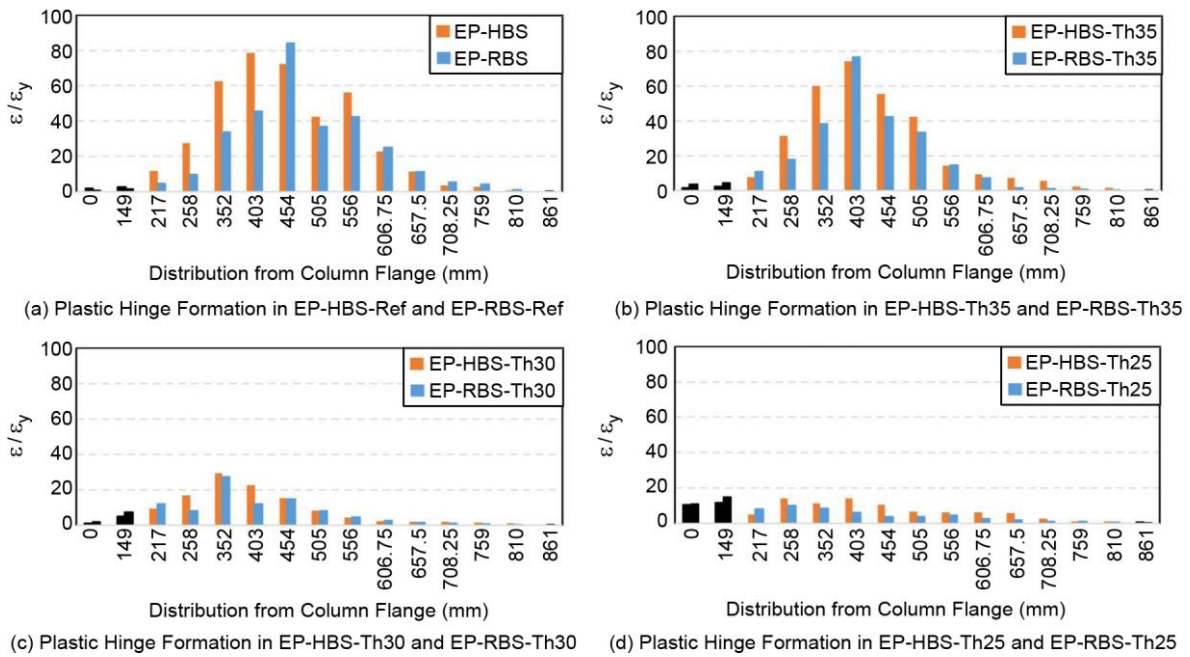


Figure 10. Longitudinal strains along the center of top flange of the beam from HBS and RBS specimens.

HBS and RBS specimens, the plastic hinge is reduced and promoted in adjacent to the end plate weld, so that, the maximum plastic strain in both techniques with a 20 mm reduction in the endplate thickness is resulted a 78% reduction compared to the reference specimens (see Figure 10b). This implies a 78% reduction in the plastic strain resulted from the low ductility in the region of the end plate weld. While, the “annealing” and “reduction” techniques were successful in shifting the plastic hinge action away from the welded joint for the endplate connections with a decrease of 15 mm in the endplate thickness (see Table 3). Moreover, the strain difference of the plastic hinge region (454 mm dis. from column face in Figure 10a) with other areas for RBS specimens is very high in compare with HBS specimens. This shows that the HBS method provides a constant reduction of material strength over entire weakened region while the strength reduction in the RBS method is concentrated in the center of trimmed flange.

4.3. Von-Mises Stress Distribution in Endplate

Figure (11) shows Von-Mises stress distribution in endplate for HBS and RBS specimens. Yielding areas of end plate are identified with gray color. As it can be seen from the figure, by

reducing the endplate thickness in HBS and RBS specimens, more areas of endplate are yielded and potential of the plastic hinge formation at the end plate is increased (due to the decrease of connection stiffness). Moreover, yielding areas of endplate for the HBS specimens are more than that for the RBS specimens. This shows RBS connections have a better performance than HBS in promoting plastic hinge far from the connection apparently. In fact, the increase in yielding area of endplate for the HBS specimens as compare to RBS caused by a constant reduction of material strength over the entire weakened region while the strength reduction in the RBS is concentrated in the center of trimmed flange. As a result of this, the concentrated strength reduction in the center of weakened region in the RBS can increase the probability of beam premature fracture in this area. Also, it can be seen from the figures, yielding area on end plate is circularly spread by decreasing the thickness of end plate. This shows the spread form of yielding area on end plate follows the arrangement pattern of the bolts.

Figure (12) shows the results of the vertical and horizontal deformations of the end plate for HBS and RBS specimens. The maximum vertical and horizontal deformation of the end plate for both HBS and RBS specimens are obtained nearly equal.

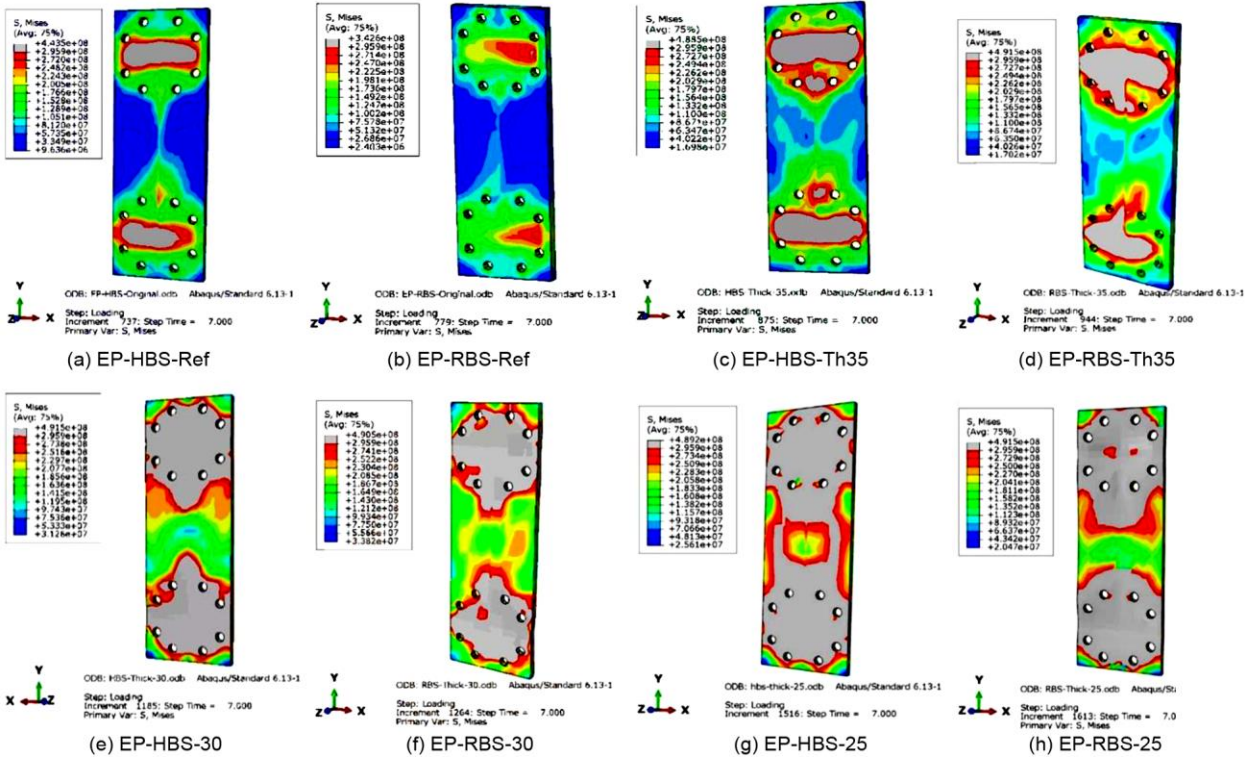


Figure 11. Von-Mises stress in end plate for HBS and RBS specimens.

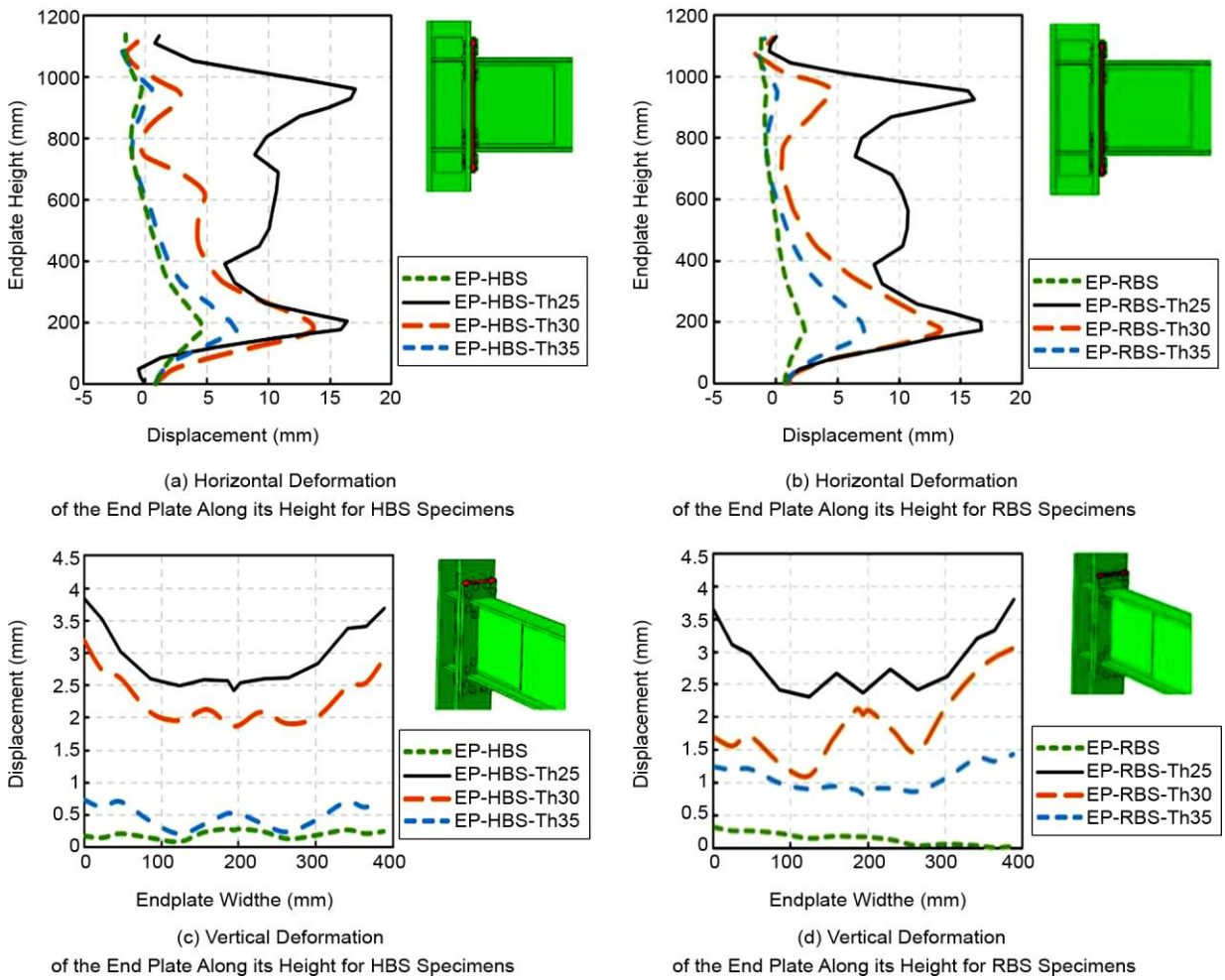


Figure 12. The curves of vertical and horizontal deformations of the end plate for HBS and RBS specimens.

It is also observed from the figure that the maximum horizontal deformation of the end plate is obtained 4.5 times more than maximum vertical deformation of that for both EP-HBS-Th25 and EP-RBS-Th25. This shows the hexagonal pattern of bolts caused the high stress concentration in the center of hexagonal pattern of the end plate holes and consequently increased the horizontal deformation in this region.

5. Comparison of “Annealing” and “Reduction” Techniques Sensitivity to the Properties of Weakened Region

Sometimes, it is probable, the implementation cases of these two techniques “annealing” and “reduction” maybe flawed. Thus, it is necessary to evaluate the sensitivity of these two techniques to the properties of weakened region. Four numerical models of HBS endplate connections with different temperature of the weakened region and four models of RBS endplate connections with different width of the trimmed area (see Figure 13b) are investigated as shown in Table (4). Ten percent reduction is considered for the properties of weakened region of the HBS and RBS specimens from each model to

next model. The presented curves (see Figure 13a) in Morrisons study [2] are used to define material properties of weakened region in different temperatures. The results of the numerical analyses are presented in three parts in the following and a brief review of the results is tabulated in Table (5).

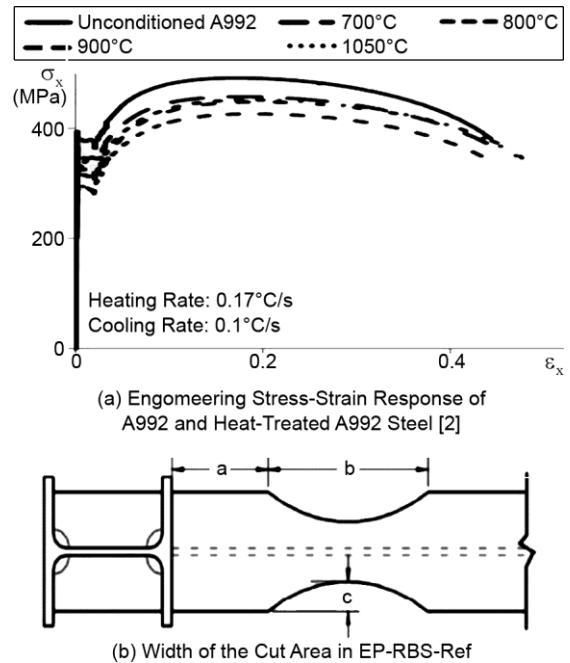


Figure 13. Numerical models details.

Table 4. Summary of the numerical model details.

Group	Specimens	a (cm)	b (cm)	c (mm)	T _{HBS} (°C)	t _{pl} (cm)
Reference Connection	EP-HBS-Ref	17.8	63.5	-	1000	45
	EP-HBS-900	17.8	63.5	-	900	45
	EP-HBS-800	17.8	63.5	-	800	45
HBS Specimens with Imperfection	EP-HBS-700	17.8	63.5	-	700	45
	EP-RBS-Ref	17.8	63.5	50	-	45
Reference Connection	EP-RBS-Ref	17.8	63.5	50	-	45
	EP-RBS-45	17.8	63.5	45	-	45
	EP-RBS-40	17.8	63.5	40	-	45
RBS Specimens with Imperfection	EP-RBS-35	17.8	63.5	35	-	45

a: Weakened area distance from column

b: Weakened area length

T_{HBS}: Weakened area temperature for HBS Connection

t_{pl}: End plate thickness

Table 5. Finite element results: moment resistance capacity, initial rotational stiffness and failure mode.

Specimens	M _{max} (KN.m)	M _{max} / M _{max(EP-HBS-Ref/EP-RBS-Ref)}	M _y (KN.m)	θ _y (rad×10 ⁻⁴)	R _m =M _y /θ _y (MN.m/rad)	θ _u (rad×10 ⁻⁴)	μ = θ _u /θ _y (rad×10 ⁻⁴)	D _m (cm)	F ^N
EP-HBS-Ref	3420	1	2235	76	294	641	8.4	41	a
EP-HBS-900	3420	1	2284	77	309	631	8.2	41	a
EP-HBS-800	3470	1.02	2268	78	324	628	8	38	a
EP-HBS-700	3660	1.07	2473	80	380	632	7.9	36	a
EP-RBS-Ref	2860	1	1833	71	220	550	7.8	75	a
EP-RBS-45	3350	1.17	2120	84	272	642	7.6	68	a
EP-RBS-40	3410	1.19	2214	86	312	620	7.2	59	a
EP-RBS-35	3510	1.23	2250	90	336	622	6.9	53	a

d: Maximum out-of-plane buckling of the beam along X axis

a: Plastic hinge in the beam

b: Plastic hinge in the end plate

N: Failure mode

5.1. Global Response of HBS and RBS Specimens

Figure (14) shows the comparison of the hysteresis curves between HBS and RBS specimens with changes in the properties of the weakened area. As it can be seen from the figure, HBS specimens with wide hysteresis loop indicating better energy dissipation in compare with RBS specimens.

Moreover, a 30% reduction in the temperature of HBS and width of the weakened region of RBS specimens caused a 7% and 25% increase in ultimate strength respectively. According to AISC 360, connections that transmit less 20% of the fully plastic moment of the beam at a rotation of 0.02 rad may be considered to have no flexural

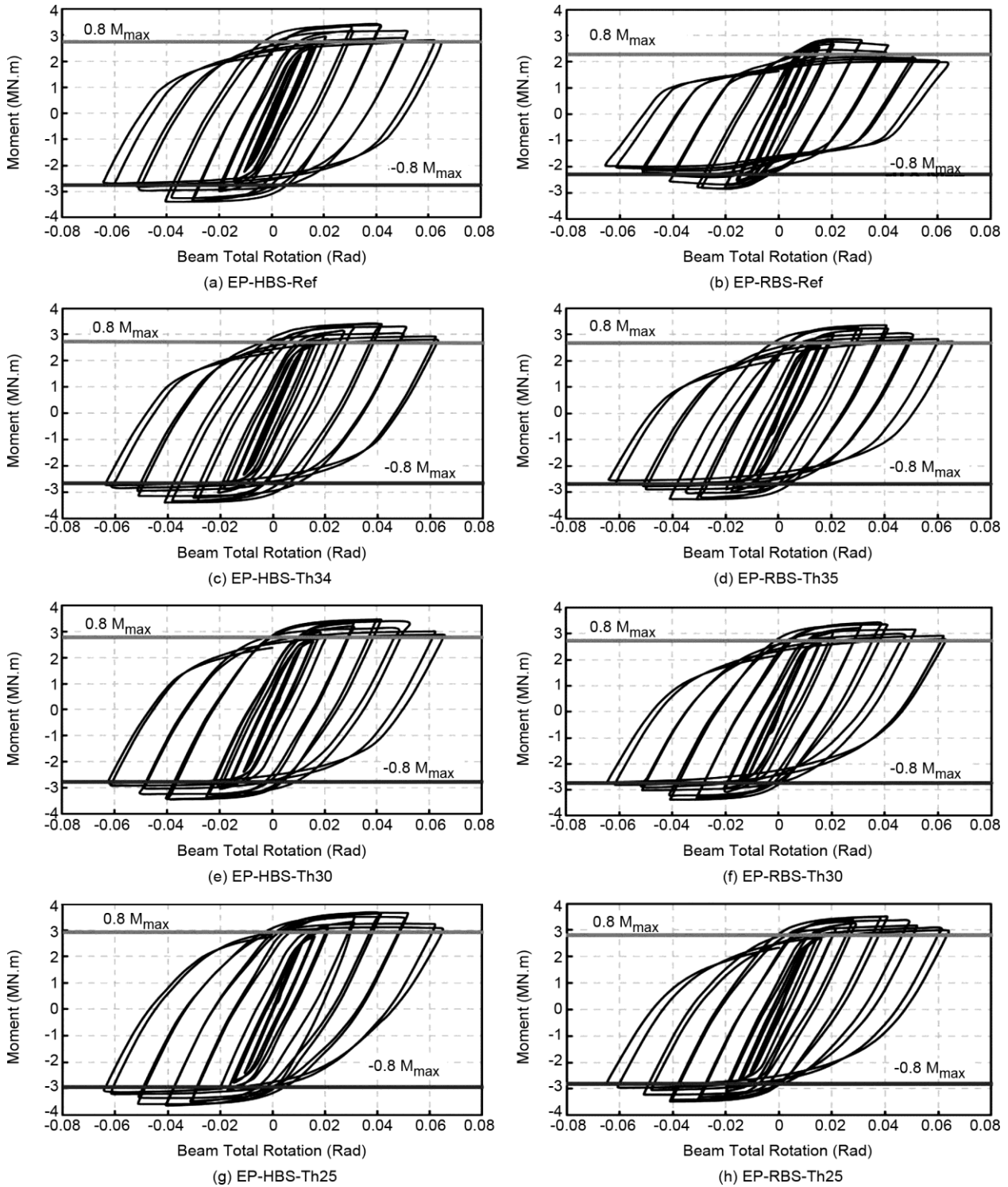


Figure 14. Hysteresis curves of HBS and RBS specimens.

strength for design [17]. The limitations of flexural strength for all specimens are presented with a line in Figure (14). However, strength degradation is within the permissible limits for all HBS and RBS specimens, and satisfies requirements of the AISC 360. From Table (5), the increase in stiffness of EP-RBS-35 relative to the reference RBS is 20% more than EP-HBS-700 relative to the reference HBS. Moreover, the decrease in ductility of EP-RBS-35 relative to the reference RBS is 6% more than EP-HBS-700 relative to the reference HBS. It can be concluded from the results, the strength, stiffness and ductility criteria of RBS specimens were more sensitive to the properties of weakened region than HBS specimens. Maximum out-of-plane buckling of the beam along X axis is presented for HBS and RBS specimens in Table (5). The comparison between HBS and RBS specimens shows that the maximum out-of-plane buckling of beam for RBS

specimens is 80% more than HBS specimens. It shows that the HBS endplate connection against local buckling of beam web and torsional instability has a better performance than RBS end plate connection.

The equivalent plastic strain of HBS and RBS specimens at the final stage of loading is shown in Figure (15). The strain variation process in specimens shows, despite a 30% reduction in the properties of the weakened region of both HBS and RBS specimen, the plastic hinge is formed in beam. Improvement action in HBS method unlike the RBS was performed by changing the properties of flange material instead of cutting beam flange. Therefore, the plastic strain in RBS specimens is concentrated in the center of trimmed beam flange, while in HBS specimens is distributed over the entire weakened region, so that, this has caused maximum equivalent plastic strain in EP-RBS-35 to be 8% more than EP-HBS-700.

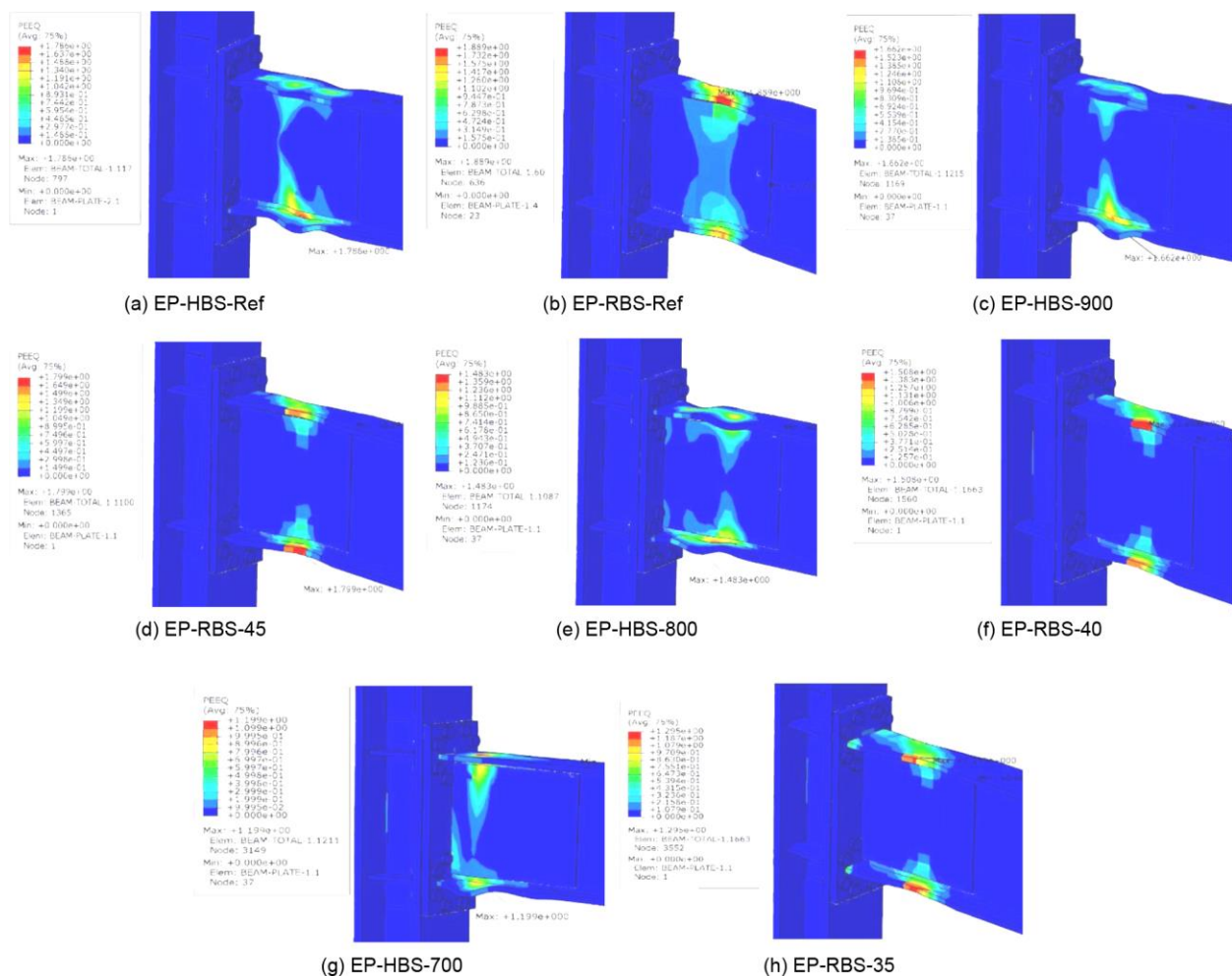


Figure 15. Equivalent plastic strain EPEQ at the final stage of loading for specimens.

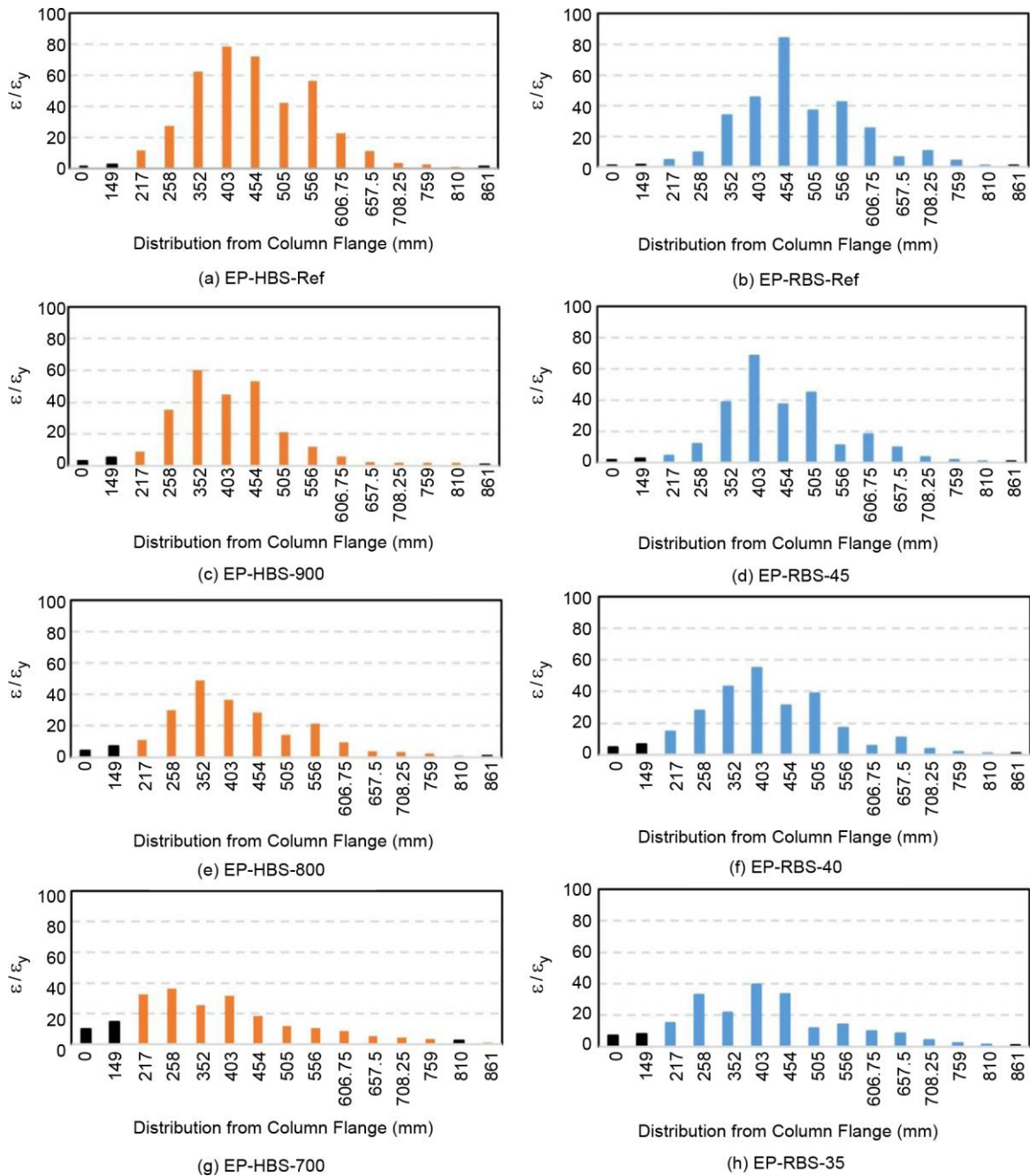


Figure 16. Longitudinal strains along the center of top flange of the beam from HBS and RBS specimens.

5.2. Plastic Hinge Formation in HBS and RBS Endplate Specimens

Figure (16) shows comparison of longitudinal tensile strains (normalized by the yield strain) along the center of top flange of the beam between HBS and RBS specimens at the end of loading. The bars highlighted in red, blue and black represent the strains in heat-treated regions in HBS specimens, reduced section of RBS specimens and non-weakened region respectively. As it can be seen from the figure, the maximum

plastic strain was decreased and tended to toward the endplate by a 30% reduction in properties of weakened region for all HBS and RBS specimens, so that, this caused the maximum plastic strain for EP-HBS-700 and EP-RBS-35 specimens relative to the reference specimens decrease 54% and 43% respectively. It shows that, the maximum strain of HBS specimens were more sensitive to the temperature of the weakened region than RBS connections to the width of the weakened region.

6. Conclusion

This study presented the comparison of “reduction” and “annealing” techniques as two improvement methods of end plate connection with an imperfection in end plate thickness. The investigation of results reveals that:

- The “annealing” technique was preferable in terms of energy dissipation, moment capacity, local buckling of beam and torsional stability.
- The two “annealing” and “reduction” techniques were successful in shifting the plastic hinge in the beam for the end-plate connections with a decrease of 15 mm in the end-plate thickness.
- The plastic hinge was formed in the column face for both EP-HBS-25 and EP-RBS25 specimens.
- The plastic strain in “reduction” specimens due to applying cut in the beam flange is concentrated in the center of trimmed flange, while the plastic strain in “annealing” specimens is distributed over a larger area of the flange.
- The two technique “annealing” and “reduction” will not work to promote plastic hinge far from column face, if the imperfection in the endplate thickness is more than 40 percent.
- For the specimens with a 20 mm reduction in end-plate thickness, the maximum stress applied to end-plate for “reduction” specimen was three times higher than “annealing” specimen.
- The strength degradation was within the permissible limits for all “annealing” and “reduction” specimens, and satisfies requirements of the AISC 360 with considering the changes in weakened area.
- The strength, stiffness and ductility criteria of “reduction” specimens were more sensitive to the properties of weakened region than “annealing” specimens.

Conflict of Interest

On behalf of all authors, the corresponding author states that there is no conflict of interest.

Reference

1. Engelhardt, M.D. and Sabol, T.A. (1994) Testing of welded steel moment connections in response to the Northridge earthquake. *Northridge Steel Update*, **1**.
2. Sophianopoulos, D.S. and Deri, A.E. (2017) Steel Beam-to-Column RBS Connections with European Profiles: I. Static Optimization. *Journal of Constructional Steel Research*, **139**, 101-109.
3. Morrison, M., Schweizer, D., and Hassan, T. (2015) An innovative seismic performance enhancement technique for steel building moment resisting connections. *Journal of Constructional Steel Research*, **109**, 34-46.
4. Uang, C.M., Yu, Q.S.K., Noel, S., and Gross, J. (2000) Cyclic testing of steel moment connections rehabilitated with RBS or welded haunch. *Journal of Structural Engineering*, **126**(1), 57-68.
5. Judd, J.P., Charney, F.A., and Pryor, S.E. (2015) Retrofit of steel-frame buildings using enhanced gravity-frame connections. *Second ATC & SEI Conference on Improving the Seismic Performance of Existing Buildings and Other Structures*, San Francisco, California.
6. Morkhade, S.G., Kshirsagar, M., Dange, R., and Patil, A. (2019) Analytical study of effect of web opening on flexural behaviour of hybrid beams. *Asian Journal of Civil Engineering*, **20**, 537-547.
7. Kim, S.Y. and Lee, C.H. (2017) Seismic retrofit of welded steel moment connections with highly composite floor slabs. *Journal of Constructional Steel Research*, **139**, 62-68.
8. Gil, B. and Goñi, R. (2015) T-stub behaviour under out-of-plane bending. I: Experimental research and finite element modelling. *Engineering Structures*, **98**, 230-240.
9. Han, S.W., Kwon, G.U., and Moon, K.H. (2007) Cyclic behaviour of post-Northridge WUF-B connections. *Journal of Constructional Steel Research*, **63**(3), 365-374.

10. Gerami, M., Saberi, H., Saberi, V., and Daryan, A.S. (2011) Cyclic behavior of bolted connections with different arrangement of bolts. *Journal of Constructional Steel Research*, **67**(4), 690-705.
11. Abidelah, A., Bouchaïr, A., and Kerdal, D.E. (2012) Experimental and analytical behavior of bolted end-plate connections with or without stiffeners. *Journal of Constructional Steel Research*, **76**, 13-27.
12. Hamburger, R.O. (2006) Prequalified Connections for Special and Intermediate Steel Moment Frames for Seismic Applications, ANSI/AISC 358-05. *Structures Congress 2006: Structural Engineering and Public Safety*, 1-8.
13. Quayyum, S. (2014) *Advanced Finite Element Analyses of Moment Resisting Connections for Improving Seismic Performance and Exploring Effects of Residual Stress and Fire Damage*. North Carolina State University.
14. ABAQUS/PRE (1997) *Manual AU*. Hibbit: Karlsson and Sorensen Inc.
15. AISC (2006) *Manual of Steel Construction Load and Resistance Factor Design*. 13th Ed. Chicago, IL.
16. SAC Joint Venture (1997) *SAC/BD-97/02 Protocol for Fabrication, Inspection, Testing and Documentation of Beam-Column Connection Tests and other Experimental Specimens*.
17. AISC (2010) *Specification for Structural Steel Buildings (ANSI/AISC 360-10)*. American Institute of Steel Construction.